

Article

Novel Low Temperature Route to Produce CdS/ZnO Composite Nanofibers as Effective Photocatalysts

Abdullah M. Al-Enizi ¹, M. M. El-Halwany ², Mohammed A. Al-Abdrabnabi ¹,
Mahmoud Bakrey ³, Mohd Ubaidullah ¹ and Ayman Yousef ^{4,5,*}

¹ Department of Chemistry, College of Science, King Saud University, Riyadh 11451, Saudi Arabia; amenizi@ksu.edu.sa (A.M.A.-E.); moh_chemical@hotmail.com (M.A.A.-A.); mtayyab@ksu.edu.sa (M.U.)

² Engineering Mathematics and Physics Department, Faculty of Engineering, Mansoura University, El-Mansoura 35516, Egypt; mmelhalwany@yahoo.com

³ Department of Engineering Materials and Design, Faculty of Energy Engineering, Aswan University, Aswan 81528, Egypt; mahmoud19742002@yahoo.com

⁴ Department of Mathematics and Physics Engineering, Faculty of Engineering at Mataria, Helwan University, Cairo 11718, Egypt

⁵ Chemical Engineering Department, Jazan University, Jazan 45142, Saudi Arabia

* Correspondence: aymanyousef84@gmail.com

Received: 3 March 2020; Accepted: 8 April 2020; Published: 10 April 2020



Abstract: In this work, CdS/ZnO composite nanofibers (NFs) were prepared by the electrospinning of a sol–gel comprised of poly(caprolactone), zinc acetate dihydrate, cadmium acetate dihydrate, and ammonium sulfide. The electrospun NF mats were calcined under vacuum in an argon (Ar) atmosphere at 200 °C for 1 h. Standard physiochemical analysis techniques demonstrated the formation of the crystalline hexagonal phase of CdS and ZnO. Composite NFs showed good photocatalytic degradation of methylene blue (MB) dye under visible light irradiation compared to their counterparts. CdS nanoparticles, ZnO nanofibers, and composite NFs photodegraded 35.5%, 47.3%, and 90% of the MB dye, respectively, within 100 min. The reaction kinetics of MB photodegradation using the composite NFs followed the pseudo-first-order relation. Owing to their facile preparation and good photodegradation ability, the proposed method can be used to prepare various photocatalysts for wastewater treatment.

Keywords: electrospinning; CdS nanoparticles; ZnO nanofibers; photocatalyst

1. Introduction

Environmental pollution is currently considered to be one of the four major global issues [1,2]. This problem is exacerbated by increasing industrial development and its use of organic pollutants, which produce high amounts of organic contaminants [1–3]. Among these, methylene blue (MB) is one of the cationic dyes. It has many industrial uses, such as dyeing of silk, leather, plastics, paper, and cotton [4]. Various chemical and physical processes have been used to treat these contaminants. Among these processes, photocatalytic degradation using semiconductor materials is considered an advanced chemical process and an effective route to reduce the environmental pollution caused by industrial organic pollutants [5,6]. Various photocatalytic semiconductors have been applied to treat organic contaminants (e.g., ZnO, TiO₂, CdS, and ZnS) [3,7–19]. Among them, nanocomposites based on ZnO and CdS have attracted special attention owing to their facile preparation in various shapes and sizes using different techniques (e.g., electrochemical deposition, hydrothermal synthesis, precipitation, and sol–gel process) [8,9,17,20–24]. In recent years, one-dimensional (1D) nanostructures have become important in various applications owing to their novel physical and chemical properties and enriched

photocatalytic activities arising from their unique geometrical structures [2,6,25–28]. Among 1D nanostructures, nanofibers (NFs) have received particular consideration owing to their high surface area, high axial ratio, good mechanical properties, and exceptional physical properties [18,19,29–31]. Moreover, compared to other nanostructures, NFs exhibit easy electron transfer, which can enhance the photodegradation process [18,32,33]. Electrospinning (ES) is the most common procedure for the production of NFs, owing to its ease, cost effectiveness, great yield, and efficiency [17,34,35]. Most of the processes used to prepare pure CdS consist of an in situ chemical process and are performed at low temperatures to prevent CdS oxidation. Guorui et al. [6] prepared 1D CdS/ZnO core/shell NFs using an ES technique for the production of hydrogen from water splitting. They calcinated electrospun NF mats in an oxygen atmosphere at high temperature to remove the poly(vinylpyrrolidone) (PVP) polymer substrate and form crystalline CdS/ZnO. However, their results indicated the formation of cadmium sulfate rather than cadmium sulfide, which could have been due to the high calcination temperature in the oxygen atmosphere. To avoid the formation of cadmium sulfate, Bishweshwar et al. [36] synthesized CdS-doped TiO₂ nanoparticle (NP)-decorated carbon NFs as a proficient photocatalyst for the removal of organic waste product. The photocatalyst was prepared at high temperature under an Ar atmosphere using PVP. They reported the formation of carbon NFs doped with pure CdS-doped TiO₂ NPs. Under these conditions, PVP converted to carbon NFs. The formed NFs mainly consisted of carbon and showed a low-light transfer to the surface of the photocatalyst. In order to overcome this issue, a low-temperature decomposition polymer and an inert atmosphere to avoid the sulfide oxidation are required.

In this study, we prepared CdS/ZnO composite NFs by the ES of a solution consisting of poly(caprolactone), zinc acetate dihydrate, cadmium acetate dihydrate, and ammonium sulfide. The electrospun NF mats were calcined under vacuum at 200 °C for 1 h. This low temperature was sufficient for removal of poly(caprolactone) and the formation of crystalline NFs. To our knowledge, no study on the use of this procedure to prepare composite NFs has been published. The prepared composite NFs exhibited good photocatalytic action in the degradation of MB dye in visible light.

2. Results and Discussions

2.1. Structure and Morphologies of the Prepared NFs

Figure 1a depicts the FE-SEM micrographs of the electrospun NFs after vacuum-drying. As exhibited in Figure 1a, the produced composite NFs are smooth and bead-free. After calcination, composite NFs are still smooth, but pearls appear in the fibers (Figure 1b). This may be due to the agglomeration of CdS NPs during calcination. The EDX analysis results shown in Figure 2 indicate that the composite NFs contain only Zn, Cd, O, and S, with contents of 73.6 wt.%, 6.9 wt.%, 17.1 wt.%, and 2.4 wt.%, respectively, as detailed in Table 1. The obtained values are close to the theoretical feed ratio, which confirm that the preparation of the composite NFs was successful.

Table 1. Elemental composition of CdS nanoparticle-doped ZnO nanofibers by EDX.

No.	Element	Weight (%)	Atomic (%)
1	O	17.1	45.9
2	S	2.4	3.2
3	Cd	6.9	2.6
4	Zn	73.6	48.3
	Total	100.0	100.0

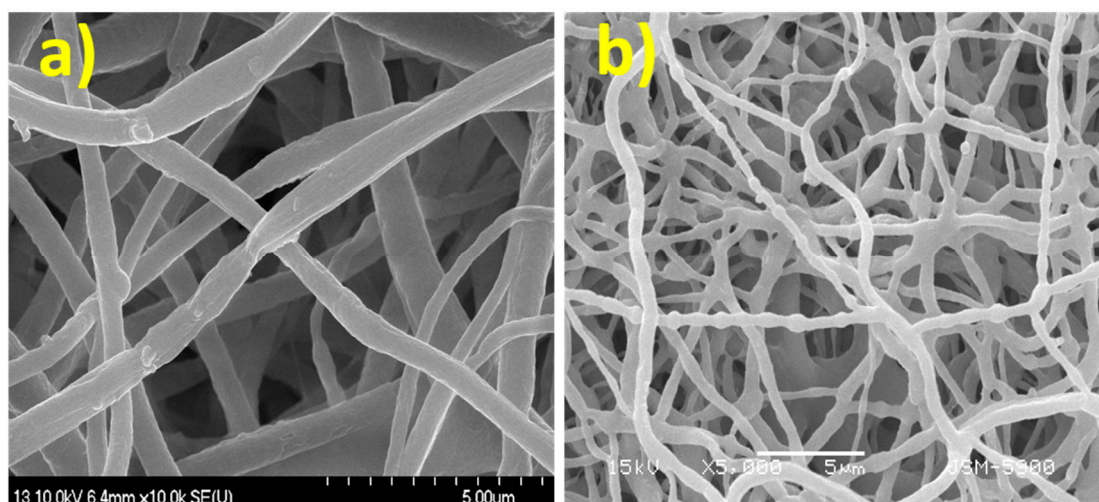


Figure 1. SEM images of the prepared composite nanofibers (NFs) (a) before calcination and (b) after calcination.

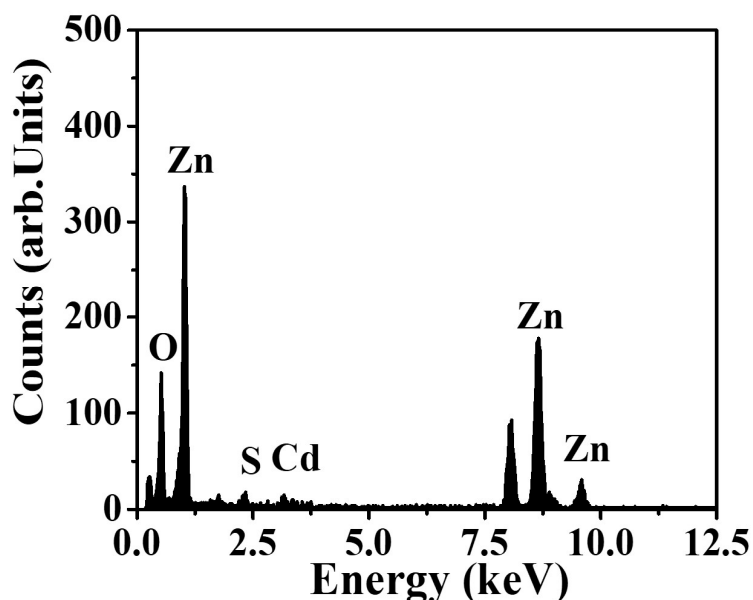


Figure 2. EDX spectrum of the prepared powder after calcination at 200 °C for 1 h.

Figure 3 shows the powder X-ray diffraction (XRD) patterns of the as-prepared ZnO NFs and composite NFs. As illustrated in Figure 3a, there are standard ZnO NFs diffraction peaks, which indicate the construction of the hexagonal wurtzite structure of ZnO (Sp.Gr P63mc (186), JCPDS 36-1451). As shown in Figure 3b, the composite NFs lead to the appearance of additional peaks corresponding to the formation of the hexagonal crystalline structure CdS (Sp.Gr Fm43m (216), JCPDS 10-454) [25,37]. Figure 4a–c shows TEM, high-resolution TEM, and TEM-EDX images of the synthesized composite NFs. As shown in Figure 4a, the NF surface is smooth. Figure 4b indicates the occurrence of clear parallel atomic planes owing to the formation of crystalline composite NFs. The indexes and labels in Figure 4b indicate clear lattice fringes on the composite NFs, where the spacings are 25 and 35 nm, corresponding to (110) plane of ZnO and (111) plane of CdS, respectively; these measurements reveal that the prepared composite NFs have excellent crystallinity. The crystallinity was confirmed by the line-EDX analysis (Figure 4a). As shown in Figure 4c, the NFs contained only Zn, Cd, O, and S, and the Cd and S have a similar distribution, confirming the formation of crystalline composite NFs.

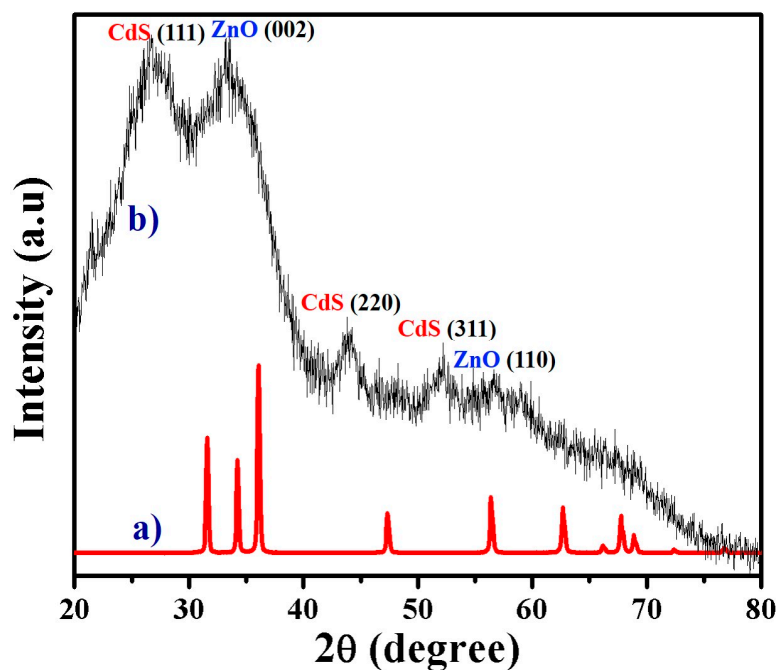


Figure 3. XRD patterns of the (a) ZnO NFs and (b) nanocomposite NFs obtained after calcination at 200 °C for 1 h.

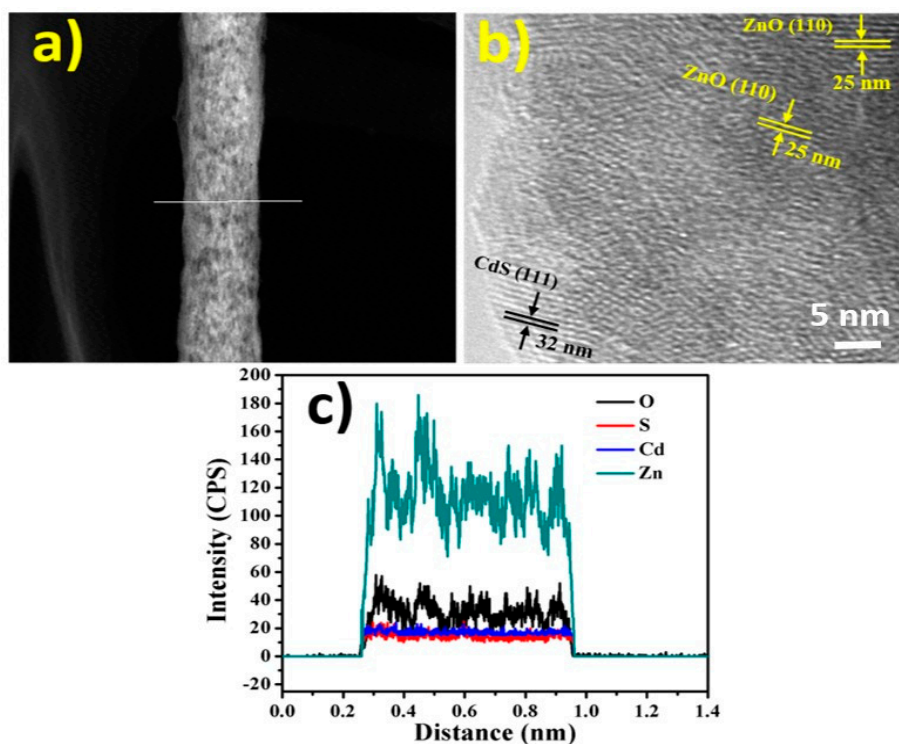


Figure 4. TEM analysis results for the calcined NFs. (a) Scanning TEM image for one NF along with the line-EDX analysis results. (b) High-resolution TEM image. (c) Line analysis for the TEM-EDX results for the line in panel (a).

Figure 5 shows the UV–Vis absorption spectra of the CdS NPs, ZnO NFs, and composite NFs. The optical band gap energies (E_g) of the CdS NPs, ZnO NFs, and composite NFs were estimated using the following equation:

$$(\alpha h\nu)^2 = A (h\nu - E_g) \quad (1)$$

where A is the proportionality constant, a is the absorption coefficient, h is Planck's constant, and ν is the frequency of light [11]. The inset in Figure 5 shows the Tauc plots, in which the E_g values were obtained by extrapolating the linear portions of the curves near the onset of the absorption edge to the energy axis. The E_g values of the CdS NPs, ZnO NFs, and composite NFs were determined to be 2.35, 3.23, and 2.45 eV, respectively, which match the values reported in the literature [2].

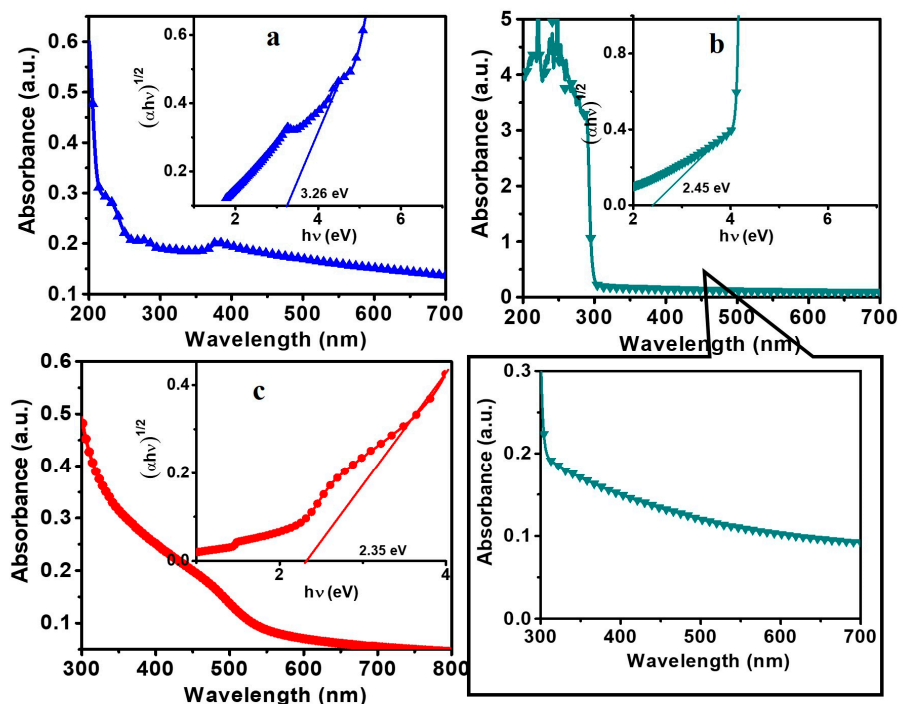


Figure 5. UV-Vis absorption spectra of the (a) ZnO NFs, (b) composite NFs, and (c) CdS nanoparticles (NPs); the insets show the Tauc plots.

2.2. Photodegradation Study

The photocatalytic performance of the composite NFs on the degradation of MB under visible light irradiation was compared to those of the pristine ZnO NFs and CdS NPs, and the results are reported in Figure 6. As shown in the figure, the photodegradation ratios of MB under visible light irradiation after 100 min were 90%, 47.3%, and 35.5% for composite NFs, ZnO NFs, and CdS NPs, respectively. Furthermore, the photodegradation ratio of MB in the absence of photocatalyst was lower than 15%. The reaction kinetics of MB photodegradation were evaluated using the following pseudo-first-order linear regression relation:

$$\ln(C_0/C) = kt \quad (2)$$

where k is the rate constant, and t indicates time. The fitting of the experimental data of $\ln C_0/C$ as a function of the degradation time yielded straight lines, and the value of k was calculated from the slope of this line. Table 2 shows the values of k obtained for the composite NFs, pristine ZnO NFs, and CdS NPs. As shown in Table 2, the obtained values of k are 0.024182, 0.005527, and 0.005297 min^{-1} for composite NFs, ZnO NFs, and CdS NPs, respectively. The high photocatalytic performance of the introduced composite NFs can be attributed to the following reasons: (1) The formation of the heterojunction between the CdS NPs and ZnO NFs led to the decrease in the band gap of ZnO, which was indicated by the faster transport of the charge carriers as a result of the decreasing recombination rate of the photogenerated electron–hole pairs, thereby increasing the number of reactive species for the MB degradation. (2) The composite NFs provide a large surface area, thereby increasing the number of active sites and consequently enhancing the interaction of photogenerated charge carriers with the

adsorbed molecules and forming hydroxyl and superoxide radicals, which can decompose the organic molecules [3,19].

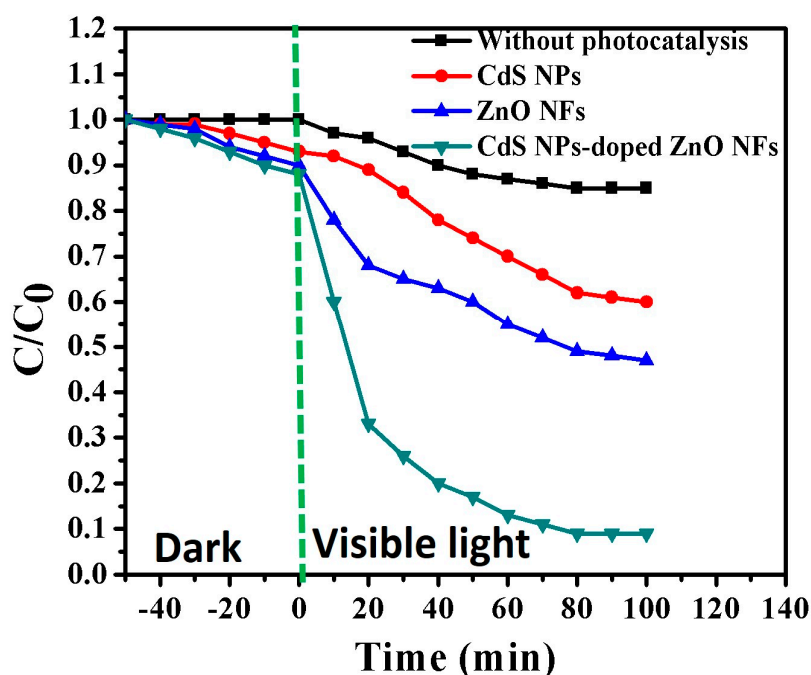


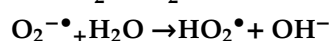
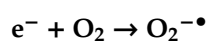
Figure 6. Comparison of the methylene blue (MB) photodegradation efficiency under visible light irradiation of the CdS NPs, ZnO NFs, and CdS NP-doped ZnO NFs.

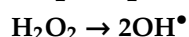
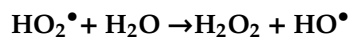
Table 2. Comparison of the values of rate constant for different photocatalysts.

No.	Photocatalyst	Rate constant (k , min^{-1})
1	Without	2.145×10^{-3}
2	CdS NPs	5.297×10^{-3}
3	ZnO NFs	5.527×10^{-3}
4	Composite NFs	2.4182×10^{-2}

Figure 7 illustrates the charge transfer and separation mechanism that supports the high photocatalytic activity of the coexistence of CdS and ZnO under visible light irradiation. The photocatalytic decolorization of MB in aqueous solution is initiated by the photoexcitation of the composite NFs under visible light leading to an easier transfer of the excited electrons from the conduction band (CB) of CdS to that of ZnO. This is due to the CB of ZnO ($E_{\text{CB}} = -4.61$ eV) being lower than that of CdS ($E_{\text{CB}} = -3.98$ eV). However, the valence band (VB) of ZnO ($E_{\text{VB}} = -7.37$ eV) is more negative than that of CdS ($E_{\text{VB}} = -6.38$ eV), which may also lead to hole transfer from the VB of ZnO to that of CdS [2,5,38]. The photogenerated holes in CdS produce hydroxyl radicals (OH^\bullet) due to the reactions of the holes in CdS with water molecules. The migrated electrons on the CB of ZnO produced superoxide radicals ($\text{O}_2^{\bullet-}$). The superoxide radicals react with holes and water and produce large numbers of hydroxyl radicals in the solution, which are considered strong oxidizing agents to decompose the organic pollutants in wastewater [39]. The photodegradation of MB under visible light mainly depends on the hydroxyl and superoxide radicals [40]. The photocatalytic degradation mechanism of the MB dye in our experiment is shown below.

At the CB





At the VB

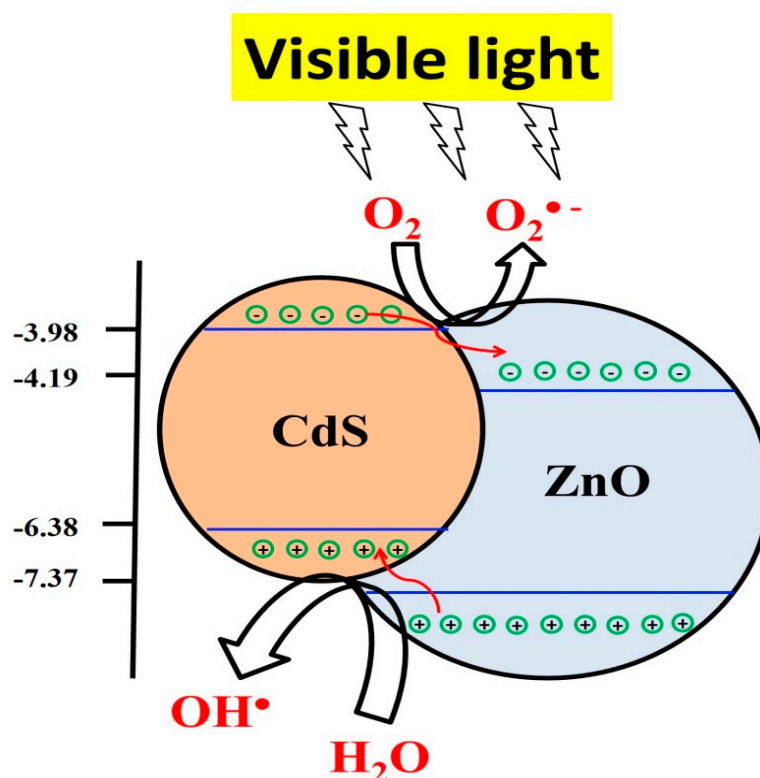


Figure 7. Schematic representation of the proposed mechanism for the photocatalysis of composite NFs.

3. Experimental

3.1. Preparation of CdS/ZnO Composite Nanofibers

The electrospun precursor solution was prepared as follows. First, 1 g $\text{Zn}(\text{CH}_3\text{COO})_2 \cdot 2\text{H}_2\text{O}$ (ZnAc, 98%, Sigma-Aldrich) was dissolved into 3 mL of *N,N*-dimethylformamide (DMF, reagent grade, 98%, Sigma-Aldrich). Second, 15 mL of 7.5 wt % poly(caprolactone) (PCL, $M_w = 80,000$ GPC, 98%, Sigma-Aldrich) was added to this solution and was stirred for 3 h at 50 °C to ensure proper mixing and form a clear sol–gel. Third, 0.1 g of $\text{Cd}(\text{CH}_3\text{COO})_2 \cdot 2\text{H}_2\text{O}$ (CdAc, 98%, Aldrich) was dissolved in 3 mL of dimethylformamide (DMF), followed by the drop-wise addition of 0.05 mL of $(\text{NH}_4)_2\text{S}$ (40–48 wt % solution in water, Sigma Aldrich) to the solution, still being stirred, to ensure the adequate distribution of cadmium sulfide (CdS) NPs. The obtained colloidal solution was stirred for a further 5 h. As reported in our previous work, lab-scale ES was used to prepare the NFs from the formed colloid solution. Typically, the formed colloidal solution was electrospun (lab scale with single-nozzle basic-level ES machine) at the high voltage of 20 kV between the needle and the rotating cylinder to charge the solution via a needle. The needle tip-to-collector distance was kept at 15 cm. The produced composite NFs were collected on a polyethylene sheet and subjected to vacuum-drying at 50 °C for 24 h, followed by heating at 200 °C for 1 h at a heating rate of 2.3 °C min^{-1} in an Ar atmosphere.

3.2. Characterization

The morphology and crystallinity of the composite NFs were analyzed using SEM (Hitachi S-7400, Tokyo, Japan) and X-ray diffraction (XRD, Rigaku Co., City, Japan), respectively. The morphology of the composite NFs was also examined by TEM (TEM-2200FS, JEOL Ltd. Tokyo, Japan) furnished with an EDX spectroscopy system functioning at 200 kV (JEOL Ltd., Tokyo, Japan) to verify the chemical structure of the composite NFs.

3.3. Photocatalytic Activity Measurements

The experiments of photodegradation of the dye solution were performed in a photoreactor (Enviolet GmbH, Karlsruhe, Germany) using a visible light source. Typically, 0.05 g of each photocatalyst was separately added to the reactor for every 100 mL of dye solution. The prepared NFs were stirred with the dye solution for 50 min before operating the light source to establish an adsorption/desorption equilibrium amongst dye molecules and the surface of the photocatalyst. A sample was taken every 2 min for analysis using a UV spectrophotometer to measure the change in the dye concentration. A control experiment without any photocatalyst was also carried out. The degradation of the MB dye was examined by measuring the difference in the absorption peak at 664 nm. The percentage of the dye that was photodegraded was measured using the following equation:

$$\text{Percentage of degradation} = (C_0 - C) / C_0 \times 100 \quad (3)$$

where C_0 is the initial dye concentration, and C is the dye concentration at time t .

4. Conclusion

We have successfully synthesized CdS/ZnO composite nanofibers from a low-degradability polymer by employing a facile electrospinning technique at low temperature under a vacuum atmosphere. The composite NFs show a good nanofibrous structure after calcination. The composite NFs consist of the crystalline hexagonal phase of CdS and ZnO. The addition of CdS NPs reduced the band gap of ZnO NFs in the composite NFs. The composite NFs showed a higher MB dye photodegradation ability under visible light than pristine ZnO NFs and CdS NPs. The reaction kinetics of MB photodegradation of the composite NFs followed the pseudo-first-order relation. Furthermore, the composite NFs showed higher rate constants compared to pristine ZnO NFs and CdS NPs. Due to its facile preparation, this method can be used to prepare efficient photocatalysts for wastewater treatment.

Author Contributions: Conceptualization, A.M.A.-E., M.U. and A.Y.; Data curation, A.Y.; Funding acquisition, A.M.A.-E. and A.Y.; Investigation, M.M.E.-H., M.A.A.-A., M.U. and A.Y.; Methodology, M.A.A.-A., M.B., M.U. and A.Y.; Project administration, A.M.A.-E.; Software, M.M.E.-H., M.B. and A.Y.; Validation, M.M.E.-H.; Writing – original draft, A.Y.; Writing – review & editing, M.U. and A.Y. All authors have read and agreed to the published version of the manuscript.

Funding: This research received no external funding

Acknowledgments: The authors would like to extend their sincere appreciation to the Deanship of Scientific Research at King Saud University for funding this research group (No. RG-1435-010).

Conflicts of Interest: The authors declare no conflict of interest.

References

1. Qi, K.; Cheng, B.; Yu, J.; Ho, W. Review on the improvement of the photocatalytic and antibacterial activities of ZnO. *J. Alloy. Compd.* **2017**, *727*, 792–820. [[CrossRef](#)]
2. Singh, S.; Neeraj, K. CdS/ZnO core/shell nano-heterostructure coupled with reduced graphene oxide towards enhanced photocatalytic activity and photostability. *Chem. Phys. Lett.* **2015**, *634*, 140–145. [[CrossRef](#)]

3. Yousef, A.; Barakat, N.A.M.; Amna, T.; Unnithan, A.R.; Al-Deyab, S.S.; Kim, H.Y. Influence of CdO-doping on the photoluminescence properties of ZnO nanofibers: Effective visible light photocatalyst for waste water treatment. *J. Lumin.* **2012**, *132*. [[CrossRef](#)]
4. El-Halwany, M.M. Study of adsorption isotherms and kinetic models for Methylene Blue adsorption on activated carbon developed from Egyptian rice hull (Part II). *Desalination* **2010**, *250*, 208–213. [[CrossRef](#)]
5. Zgura, I.; Preda, N.; Socol, G.; Ghica, C.; Ghica, D. Wet chemical synthesis of ZnO-CdS composites and their photocatalytic activity. *Mater. Res. Bull.* **2018**, *99*, 174–181. [[CrossRef](#)]
6. Yang, G.; Yan, W.; Zhang, Q.; Ding, S.; Shen, S. One-dimensional CdS/ZnO core/shell nanofibers via single-spinneret electrospinning: tunable morphology and efficient photocatalytic hydrogen production. *Nanoscale. Nanoscale* **2013**. [[CrossRef](#)]
7. Yousef, A.; Barakat, N.A.M.; Al-Deyab, S.S.; Nirmala, R.; Pant, B.; Kim, H.Y. Encapsulation of CdO/ZnO NPs in PU electrospun nanofibers as novel strategy for effective immobilization of the photocatalysts. *Colloids Surfaces A Physicochem. Eng. Asp.* **2012**, *401*. [[CrossRef](#)]
8. Luo, Y. Hydrothermal synthesis of one-dimensional ZnO/CdS core/shell nanocomposites. *Colloid J.* **2009**, *71*, 370–374. [[CrossRef](#)]
9. Arunraja, L.; Thirumoorthy, P.; Karthik, A.; Subramanian, R.; Rajendran, V. Investigation and characterization of ZnO/CdS nanocomposites using chemical precipitation method for gas sensing applications. *J. Mater. Sci. Mater. Electron.* **2017**, *28*, 18113–18120. [[CrossRef](#)]
10. Su, B.; Zhong, M.; Han, L.; Wei, M.; Liu, Y.; Yang, H.; Lei, Z. Eco-friendly preparation of hierarchically self-assembly porous ZnO nanosheets for enhanced photocatalytic performance. *Mater. Res. Bull.* **2020**, *124*, 110777. [[CrossRef](#)]
11. Keerthana, B.G.T.; Murugakoothan, P. Synthesis and characterization of CdS/TiO₂ nanocomposite: Methylene blue adsorption and enhanced photocatalytic activities. *Vacuum* **2019**, *159*, 476–481. [[CrossRef](#)]
12. Franco, A.; Neves, M.C.; Carrott, M.R.; Mendonça, H.; Pereira, M.I.D.S.; Monteiro, O. Photocatalytic decolorization of methylene blue in the presence of TiO₂/ZnS nanocomposites. *J. Hazard. Mater.* **2009**, *161*, 545–550. [[CrossRef](#)] [[PubMed](#)]
13. Cao, Z.; Zhang, T.; Ren, P.; Cao, D.; Lin, Y.; Wang, L.; Zhang, B.; Xiang, X. Doping of Chlorine from a Neoprene Adhesive Enhances Degradation Efficiency of Dyes by Structured TiO₂-Coated Photocatalytic Fabrics. *Catalysts* **2020**, *10*. [[CrossRef](#)]
14. Peng, J.; Lu, T.; Ming, H.; Ding, Z.; Yu, Z.; Zhang, J.; Hou, Y. Enhanced Photocatalytic Ozonation of Phenol by Ag/ZnO Nanocomposites. *Catalysts* **2019**, *9*. [[CrossRef](#)]
15. Guo, J.; Khan, S.; Cho, S.-H.; Kim, J. Preparation and immobilization of zinc sulfide (ZnS) nanoparticles on polyvinylidene fluoride pellets for photocatalytic degradation of methylene blue in wastewater. *Appl. Surf. Sci.* **2019**, *473*, 425–432. [[CrossRef](#)]
16. Soltani, N.; Saion, E.; Hussein, M.Z.; Erfani, M.; Abedini, A.; Bahmanrokh, G.; Navasery, M.; Vaziri, P. Visible Light-Induced Degradation of Methylene Blue in the Presence of Photocatalytic ZnS and CdS Nanoparticles. *Int. J. Mol. Sci.* **2012**, *13*, 12242–12258. [[CrossRef](#)]
17. Afeesh, R.; Barakat, N.A.; Al-Deyab, S.S.; Yousef, A.; Kim, H.Y. Nematic shaped cadmium sulfide doped electrospun nanofiber mat: Highly efficient, reusable, solar light photocatalyst. *Colloids Surfaces A: Physicochem. Eng. Asp.* **2012**, *409*, 21–29. [[CrossRef](#)]
18. Yousef, A.; Barakat, N.A.; Kim, H.Y. Electrospun Cu-doped titania nanofibers for photocatalytic hydrolysis of ammonia borane. *Appl. Catal. A: Gen.* **2013**, *467*, 98–106. [[CrossRef](#)]
19. Yousef, A.; Barakat, N.A.; Amna, T.; Al-Deyab, S.S.; Hassan, M.S.; Abdal-Hay, A.; Kim, H.Y. Inactivation of pathogenic *Klebsiella pneumoniae* by CuO/TiO₂ nanofibers: A multifunctional nanomaterial via one-step electrospinning. *Ceram. Int.* **2012**, *38*, 4525–4532. [[CrossRef](#)]
20. Li, H.; Yao, C.; Meng, L.; Sun, H.; Huang, J.; Gong, Q. Photoelectrochemical performance of hydrogenated ZnO/CdS core-shell nanorod arrays. *Electrochimica Acta* **2013**, *108*, 45–50. [[CrossRef](#)]
21. Yang, Q.; Li, Y.; Hu, Z.; Duan, Z.; Liang, P.; Sun, J.; Xu, N.; Wu, J. Extended photo-response of ZnO/CdS core/shell nanorods fabricated by hydrothermal reaction and pulsed laser deposition. *Opt. Express* **2014**, *22*, 8617–8623. [[CrossRef](#)] [[PubMed](#)]

22. Yousef, A.; Barakat, N.A.; Khalil, K.A.; Unnithan, A.R.; Panthi, G.; Pant, B.; Kim, H.Y. Photocatalytic release of hydrogen from ammonia borane-complex using Ni(0)-doped TiO₂/C electrospun nanofibers. *Colloids Surfaces A: Physicochem. Eng. Asp.* **2012**, *410*, 59–65. [CrossRef]
23. Salam, S.; Islam, M.; Alam, M.; Akram, M.A.; Ikram, M.; Mahmood, A.; Khan, M.; Mujahid, M. The effect of processing conditions on the structural morphology and physical properties of ZnO and CdS thin films produced via sol-gel synthesis and chemical bath deposition techniques. *Adv. Nat. Sci. Nanosci. Nanotechnol.* **2011**, *2*, 45001. [CrossRef]
24. Optical and Microstructural Characterization of CdS–ZnO Nanocomposite Thin Films Prepared by Sol–Gel Technique—IOPscience. Available online: <https://iopscience.iop.org/article/10.1088/0022-3727/37/4/014/meta> (accessed on 27 March 2020).
25. Zou, X.; Wang, P.-P.; Li, C.; Zhao, J.; Wang, D.; Asefa, T.; Li, G.-D. One-pot cation exchange synthesis of 1D porous CdS/ZnO heterostructures for visible-light-driven H₂ evolution. *J. Mater. Chem. A* **2014**, *2*, 4682–4689. [CrossRef]
26. Zhu, Y.F.; Zhou, L.; Jiang, Q.S. One-dimensional ZnO nanowires grown on three-dimensional scaffolds for improved photocatalytic activity. *Ceram. Int.* **2020**, *46*, 1158–1163. [CrossRef]
27. Liang, H.; Bai, J.; Xu, T.; Li, C. Controllable growth of foxtail-like MoS₂ on one-dimensional carbon nanofibers with enhanced photocatalytic activity. *Vacuum* **2020**, *172*, 109059. [CrossRef]
28. Wang, Y.; Sunarso, J.; Zhao, B.; Ge, C.; Chen, G. One-dimensional BiOBr nanosheets/TiO₂ nanofibers composite: Controllable synthesis and enhanced visible photocatalytic activity. *Ceram. Int.* **2017**, *43*, 15769–15776. [CrossRef]
29. Yousef, A.; El-Halwany, M.; Barakat, N.A.; Kim, H.Y. One pot synthesis of Cu-doped TiO₂ carbon nanofibers for dehydrogenation of ammonia borane. *Ceram. Int.* **2015**, *41*. [CrossRef]
30. Zaher, A.; El Rouby, W.M.A.; Barakat, N.A. Influences of tungsten incorporation, morphology and calcination temperature on the electrocatalytic activity of Ni/C nanostructures toward urea elimination from wastewaters. *Int. J. Hydrogen Energy* **2020**, *45*, 8082–8093. [CrossRef]
31. Yousef, A.; Brooks, R.M.; El-Halwany, M.; Barakat, N.A.; El-Newehy, M.H.; Kim, H.Y. Cu₀-decorated, carbon-doped rutile TiO₂ nanofibers via one step electrospinning: Effective photocatalyst for azo dyes degradation under solar light. *Chem. Eng. Process. Process. Intensif.* **2015**, *95*. [CrossRef]
32. Yousef, A.; Brooks, R.M.; El-Newehy, M.H.; Al-Deyab, S.S.; Kim, H.Y. Electrospun Co-TiC nanoparticles embedded on carbon nanofibers: Active and chemically stable counter electrode for methanol fuel cells and dye-sensitized solar cells. *Int. J. Hydrogen Energy* **2017**, *42*. [CrossRef]
33. Yousef, A.; Brooks, R.M.; El-Halwany, M.; Abutaleb, A.; El-Newehy, M.H.; Al-Deyab, S.S.; Kim, H.Y. Electrospun CoCr 7 C 3-supported C nanofibers: Effective, durable, and chemically stable catalyst for H₂ gas generation from ammonia borane. *Mol. Catal.* **2017**, *434*. [CrossRef]
34. Brooks, R.M.; Maafa, I.M.; Al-Enizi, A.M.; El-Halwany, M.M.; Ubaidullah, M.; Yousef, A. Electrospun Bimetallic NiCr Nanoparticles@Carbon Nanofibers as an Efficient Catalyst for Hydrogen Generation from Ammonia Borane. *Nanomaterial* **2019**, *9*. [CrossRef] [PubMed]
35. Panthi, G.; Yousef, A.; Barakat, N.A.; Khalil, K.A.; Akhter, S.; Choi, Y.R.; Kim, H.Y. Mn₂O₃/TiO₂ nanofibers with broad-spectrum antibiotics effect and photocatalytic activity for preliminary stage of water desalination. *Ceram. Int.* **2013**, *39*. [CrossRef]
36. Pant, B.; Barakat, N.A.; Pant, H.R.; Park, M.; Saud, P.S.; Kim, J.-W.; Kim, H.Y. Synthesis and photocatalytic activities of CdS/TiO₂ nanoparticles supported on carbon nanofibers for high efficient adsorption and simultaneous decomposition of organic dyes. *J. Colloid Interface Sci.* **2014**, *434*, 159–166. [CrossRef] [PubMed]
37. Bu, Y.; Chen, Z.; Li, W.; Yu, J. High-Efficiency Photoelectrochemical Properties by a Highly Crystalline CdS-Sensitized ZnO Nanorod Array. *ACS Appl. Mater. Interfaces* **2013**, *5*, 5097–5104. [CrossRef]
38. The Absolute Energy Positions of Conduction and 253—Google Scholar. Available online: https://scholar.google.com/scholar?hl=en&as_sdt=0%2C5&q=The+absolute+energy+positions+of+conduction+and+253+valence+bands+of+selected+semiconducting+minerals&btnG= (accessed on 28 March 2020).

39. Velanganni, S.; Pravinraj, S.; Immanuel, P.; Thiruneelakandan, R. Nanostructure CdS/ZnO heterojunction configuration for photocatalytic degradation of Methylene blue. *Phys. B: Condens. Matter* **2018**, *534*, 56–62. [[CrossRef](#)]
40. Chaengchawi, P.; Serivalsatit, K.; Sujaridworakun, P. Synthesis of Visible-Light Responsive CdS/ZnO Nanocomposite Photocatalysts via Simple Precipitation Method. *Key Eng. Mater.* **2014**, *608*, 224–229. [[CrossRef](#)]



© 2020 by the authors. Licensee MDPI, Basel, Switzerland. This article is an open access article distributed under the terms and conditions of the Creative Commons Attribution (CC BY) license (<http://creativecommons.org/licenses/by/4.0/>).